Downloaded from jnm.snmjournals.org by on March 14, 2017. For personal use only.

Prognostic Significance of Dynamic ^{18}F-FET PET in Newly Diagnosed Astrocytic High-Grade Glioma

Nathalie L. Jansen[1], Bogdana Suchorska[2], Vera Wenter[1], Christine Schmid-Tannwald[3], Andrei Todica[1], Sabina Eigenbrod[4], Maximilian Niyazi[5], Jörg-Christian Tonn[2], Peter Bartenstein[1], Friedrich-Wilhelm Kreth[2], and Christian la Fougère[6]

[1]*Department of Nuclear Medicine, Ludwig-Maximilians-University of Munich, Germany;* [2]*Department of Neurosurgery, Ludwig-Maximilians-University, Munich, Germany;* [3]*Institute for Clinical Radiology, Ludwig-Maximilians-University, Munich, Germany;* [4]*Department of Neuropathology, Ludwig-Maximilians-University, Munich, Germany;* [5]*Department of Radiation Oncology, Ludwig-Maximilians-University, Munich, Germany; and* [6]*Division of Nuclear Medicine and Clinical Molecular Imaging, Department of Radiology, University of Tübingen, Tübingen, Germany*

Despite advances in diagnosis and the use of different therapeutic regimens in astrocytic high-grade glioma (HGG), the prognosis for patients remains grim. Additional pretherapeutic information is needed to tailor management. To gain additional prognostic information at primary diagnosis, we investigated the value of dynamic *O*-(2-^{18}F-fluoroethyl)-L-tyrosine (^{18}F-FET) PET. **Methods:** We retrospectively evaluated 121 patients who had a primary diagnosis of astrocytic HGG (51 World Health Organization [WHO] grade III; 70 WHO IV) and underwent dynamic ^{18}F-FET PET before histopathologic assessment. We assessed static parameters (maximal and mean tumoral standardized uptake value corrected for mean background activity in the contralateral hemisphere [SUV_{max}/BG and SUV_{mean}/BG, respectively], biologic tumor volume) and dynamic time–activity curves, including minimal time to peak (TTP_{min}). The prognostic influence of PET parameters and other clinical parameters on progression-free and overall survival was evaluated using uni- and multivariate Cox regression and Kaplan–Meier survival estimates. **Results:** In the group overall, median progression-free survival and overall survival were 12.2 and 21.9 mo. SUV_{max}/BG, SUV_{mean}/BG, and biologic tumor volume were significantly higher in WHO IV than in WHO III gliomas; median TTP_{min} was 12.5 min in both groups. On univariate analysis, the factors age, WHO grade, O6-methylguanine-DNA methyltransferase promoter methylation status, contrast enhancement, initial treatment, and TTP_{min} showed prognostic significance, with WHO grade, O6-methylguanine-DNA methyltransferase status, age, and TTP_{min} remaining significant in the multivariate analysis. WHO grade and TTP_{min} reached a similar fit for the prognostic evaluation. The prognosis of WHO III astrocytoma with an early TTP_{min} of 12.5 min or less did not differ significantly from that of glioblastoma. **Conclusion:** Early TTP_{min} is associated with worse outcome in patients with newly diagnosed astrocytic HGG. In the preoperative setting, TTP_{min} can be a valuable noninvasive prognostic marker with comparable significance to WHO grade. Additionally, TTP_{min} can help identify highly aggressive WHO III astrocytoma tumors and may help in adjusting standard treatment toward an individualized, risk-adapted therapy regime.

Key Words: high-grade glioma; ^{18}F-FET PET; kinetic analysis; prognostic value

J Nucl Med 2015; 56:9–15
DOI: 10.2967/jnumed.114.144675

Management of astrocytic high-grade glioma (HGG) has changed during the last 10 years. The introduction of radiotherapy plus concomitant and adjuvant temozolomide, for example, has significantly improved the prognosis of patients with glioblastoma (World Health Organization [WHO] grade IV) (*1,2*); for WHO III astrocytoma, therapeutic management is more variable and chosen individually (*3–7*). Current treatment recommendations vary: resection or biopsy followed by radio- or chemotherapy or combined-modality treatment (*8*). In consideration of the variable disease course in WHO III astrocytoma patients, with some patients presenting a rapidly progressing clinical course that does not differ significantly from glioblastoma patients, the identification of prognostic markers would be most helpful for treatment stratification.

In the last few years, O6-methylguanine-DNA methyltransferase (*MGMT*) promoter methylation and mutations in the cytosolic isocitrate dehydrogenase 1 or 2 gene have been identified as molecular–genetic factors with a favorable prognosis in astrocytic HGG, whereas loss of heterozygosity on chromosomes 1p and 19q is highly correlated with an oligodendroglial morphology (*9–11*). Beside molecular–genetic biomarker profiles, which can be assessed invasively only, molecular imaging including PET with radiolabeled amino acids or their analogs is increasingly used for tumor characterization and prognostic evaluation (*12–14*). Their potential as imaging-derived, noninvasive biomarkers is currently under investigation.

One of the most promising radiotracers is *O*-(2-^{18}F-fluoroethyl)-L-tyrosine (^{18}F-FET), which shows high uptake in glioma cells and low uptake in healthy brain tissue, resulting in an excellent tumor-to-background contrast (*15*). In this context, dynamic acquisition of ^{18}F-FET PET has gained increasing interest, as it enables glioma characterization by differentiating between low-grade gliomas (LGG) and high-grade gliomas (HGG) by analysis of individual time–activity curves of ^{18}F-FET uptake (*16–19*). These time–activity curves are typically increasing in LGG and decreasing in HGG. However, decreasing time–activity curves were recently also observed in histologically verified LGG, indicating a higher risk for

Received Jun. 25, 2014; revision accepted Dec. 2, 2014.
For correspondence or reprints contact: Nathalie Jansen, Department of Nuclear Medicine, LMU, Marchioninistrasse 15, 81377 Munich, Germany.
E-mail: nathalie.jansen@med.uni-muenchen.de
Published online Dec. 23, 2014.
COPYRIGHT © 2015 by the Society of Nuclear Medicine and Molecular Imaging, Inc.

Downloaded from jnm.snmjournals.org by on March 14, 2017. For personal use only.

poor outcome (*20*). Another study has reported a characteristic change in time–activity curves during malignant transformation of low-grade to high-grade astrocytoma (*21*).

In the current retrospective study, we aimed to identify dynamic ^{18}F-FET PET parameters associated with tumor aggressiveness in patients with newly diagnosed, histologically confirmed astrocytic HGG. We focused on time–activity curve patterns and more specifically on the prognostic impact of the time to maximal ^{18}F-FET uptake.

MATERIALS AND METHODS

Patient Evaluation

We retrospectively identified patients with a newly diagnosed WHO III or IV supratentorial astrocytic glioma who had undergone dynamic ^{18}F-FET PET before histologic diagnosis at the Ludwig-Maximilians-University of Munich between 2004 and 2012. Patients with an oligoastrocytoma or oligodendroglioma were excluded to ensure homogeneity in the patient collective. The study was approved by the institutional review board, and all subjects gave written informed consent. The primary endpoint of the study was overall survival (OS), and the secondary endpoint was progression-free survival (PFS). PFS was calculated from the baseline PET scan to the first event of clinical deterioration, that is, new neurologic symptoms, worsening as indicated by Karnofsky performance score or an increase in administered steroid medication, or tumor growth on conventional MR imaging. OS was correspondingly measured from baseline PET scan to date of death. The date of last follow-up was November 2013.

^{18}F-FET PET and MR Imaging

Dynamic ^{18}F-FET PET scans were acquired with an ECAT EXACT HR+ scanner (Siemens Healthcare) according to standard protocols (*20*) after a slow intravenous bolus injection of 180 MBq of ^{18}F-FET. Dynamic emission was recorded in 3-dimensional mode for 16 frames (7 × 10 s, 3 × 30 s, 1 × 2 min, 3 × 5 min, and 2 × 10 min) until 40 min after injection. For further evaluation, the images were transferred to a Hermes workstation (Hermes Medical Solutions).

Semiquantitative evaluation included maximal tumoral standardized uptake value corrected for mean background activity in the contralateral hemisphere (SUV_{max}/BG) and an estimated biologic tumor volume (BTV) defined by semiautomatic threshold-based calculation of a volume of interest (SUV/BG ≥ 1.8). Furthermore, mean tracer uptake within the BTV (SUV_{mean}/BG) was assessed.

For dynamic evaluation of ^{18}F-FET uptake, a 90% isocontour threshold region of interest was defined on the 10- to 30-min summation images (frames 13–15) on each individual slice throughout the tumor and applied to the dynamic PET data to extract the time–activity curves. Because of low counting rates and the risk of noise artifacts in the very early time frames, only frames 11–16 (3–40 min) were considered for further analysis. For each slice within the tumor, the frame with the peak uptake was identified. The starting time of the frame plus half the frame duration, corresponding to the respective peak value, was set as time to peak (TTP). Accordingly, TTP accounted for 4 min in frame 11, 7.5 min in frame 12, 12.5 min in frame 13, 17.5 min in frame 14, 25 min in frame 15, and 35 min in frame 16 (Fig. 1). The shortest TTP present in at least 2 adjacent slices was defined as minimal TTP (TTP_{min}).

MR imaging was performed before tissue sampling according to standard protocols (*19*), which included acquisition of axial T2-weighted sequences and 3-dimensional T1-weighted sequences before and after administration of intravenous contrast agent (gadobenate dimeglumine, 0.1 mmol/kg [MultiHance; Bracco Imaging]). The presence of contrast enhancement was evaluated as a factor for further analyses.

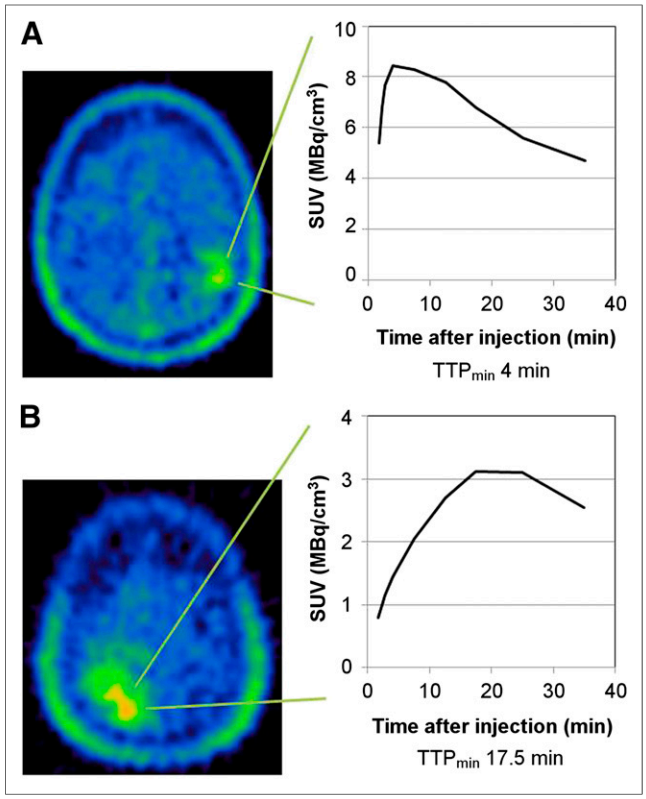


FIGURE 1. Time–activity curves of ^{18}F-FET uptake were evaluated slice by slice throughout entire tumor to assess TTP_{min}. (A) Example of decreasing curve with early peak after 4 min. (B) Example of late peak after 17.5 min.

Stereotactic Biopsies, Microsurgical Resections, and Histologic Evaluation

Tissue specimens for histologic and molecular–genetic evaluation were obtained by either serial stereotactic biopsy or resection. Microsurgical resections were performed by experienced neurosurgeons using neuronavigation with MR imaging and PET image fusion (Brainlab). Molecular stereotactic biopsy procedures were performed as published in detail previously (*19,22*). A biopsy sample with an average tissue volume of approximately 1 mm^3 was obtained from the area of highest ^{18}F-FET uptake. The mean number of obtained tumor samples per patient was 5. Histologic classification and tumor grading were performed according to the current WHO guidelines at the respective time point of histopathologic assessment (*23*). The German Brain Tumor Reference in Bonn was consulted for complex cases. Determination of *MGMT* promoter methylation was performed using methylation-specific polymerase chain reaction according to standard protocols (*24*).

Statistical Analysis

SPSS (version 21.0; IBM) for Windows (Microsoft) was used for statistical calculations. Length of OS and PFS was analyzed with the Kaplan–Meier method. The distribution of patient- and tumor-related variables was analyzed by χ^2 statistics (for categoric variables) and Mann–Whitney *U* testing (for continuously scaled variables). Continuous parameters were reported as mean ± SD and range. The median was used as the threshold for dichotomization of parameters. For univariate prognostic analyses, all parameters were evaluated using Cox regression. The covariates that proved significant in 1-variable models were then evaluated in multivariate analyses using a stepwise backward exclusion model. When there was an intercorrelation of the

Downloaded from jnm.snmjournals.org by on March 14, 2017. For personal use only.

most relevant covariates, alternative models were tested and were compared by computing the maximized likelihoods. A 2-tailed P value of less than 0.05 was considered significant.

RESULTS

In total, 121 patients (73 men and 48 women; mean age, 54.0 ± 13.7 y) with a primary diagnosis of astrocytic HGG were included (51 WHO III astrocytomas and 70 WHO IV glioblastomas). The median Karnofsky performance score was 90 (range, 60–90; only one patient with a Karnofsky performance score of 60); 88 patients underwent stereotactic biopsy and 33 patients microsurgical resection. Detailed results of the clinical parameters, including treatment, are listed in Table 1.

In the ^{18}F-FET PET scan, 116 of 121 HGGs (>95%) showed enhanced ^{18}F-FET uptake. Five WHO III astrocytomas, however, were found to be ^{18}F-FET–negative. SUV_{max}/BG and SUV_{mean}/BG were higher in glioblastomas than in WHO III tumors (3.7 vs. 3.0, $P < 0.01$, and 2.3 vs 2.1, $P < 0.01$), and glioblastomas exhibited larger BTVs (25.5 vs. 13.1 mL, $P < 0.01$). Kinetic analysis was available for 111 of 116 ^{18}F-FET–positive patients (43 WHO III and 68 WHO IV); in 10 patients kinetic analysis was not available (5 for technical reasons, 5 because of absence of ^{18}F-FET uptake). The median TTP_{min} in both WHO groups was 12.5 min. In the WHO III group, 22 of 43 patients (51%) had a TTP_{min} of 12.5 min or less (including 10 patients without contrast enhancement on MR imaging); in the glioblastoma group, 50 of 68 patients (74%) had a TTP_{min} of 12.5 min or less (Table 1). TTP_{min} was intercorrelated with WHO grade ($P = 0.02$).

During follow-up (median for survivors, 61.3 mo; range, 7.2–101.9 mo), 98 of 121 patients experienced tumor progression (35 WHO III and 63 WHO IV) and 88 of 121 patients died (26 WHO III and 62 WHO IV).

Median PFS and OS for the entire study group were 12.2 and 21.9 mo, respectively. Patients with WHO III tumors exhibited both longer PFS and longer OS than glioblastoma patients (46.2 vs. 14.2 mo and 19.3 vs. 10.3 mo, $P \leq 0.001$).

TABLE 1
Overview of Clinical and FET PET Parameters According to WHO Group

Parameter	All HGG	WHO III	WHO IV	*P*
Patients (*n*)	121	51	70	NS
Age (y)	54.0	46.9	59.1	≤0.001
Sex				
Male (*n*)	73	32	41	NS
Female (*n*)	48	19	29	
MGMT				
Methylated (*n*)	66	33	33	0.022
Unmethylated (*n*)	43	12	31	
Not available (*n*)	12	6	6	
Contrast enhancement on MR imaging				
Yes (*n*)	95	25	70	≤0.001
No (*n*)	26	26	0	
Surgical resection (*n*)	33	6	27	≤0.001
Radiochemotherapy* (*n*)	82	17	65	≤0.001
Chemotherapy† (*n*)	23	21	2	≤0.001
Radiotherapy (60 Gy) (*n*)	13	11	2	≤0.001
Brachytherapy (*n*)	2	2	0	NS
Palliative treatment (*n*)	1	0	1	NS
^{18}F-FET PET parameters				
SUV_{max}/BG	3.4 ± 0.1	3.0 ± 0.2	3.7 ± 0.1	0.004
SUV_{mean}/BG	2.2 ± 0.1	2.1 ± 0.1	2.3 ± 0.1	0.008
BTV (mL)	20.6 ± 1.9	13.1 ± 2.6	25.5 ± 2.6	0.002
TTP_{min}				
≤12.5 min (*n*)	72	22	50	0.016
>12.5 min (*n*)	39	21	18	
Not available (*n*)	10	8	2	

NS = not statistically significant.

*Radiotherapy with concomitant and adjuvant temozolomide (60 Gy; 75 mg/m^2 of body surface area, 5 of 7 d per week, 6 wk) according to the European Organisation for Research and Treatment of Cancer and the National Cancer Institute of Canada (*1,2*).

†19 temozolomide, 4 vincristine.

Downloaded from jnm.snmjournals.org by on March 14, 2017. For personal use only.

TABLE 2
P Values for Determination of Prognostic Factors Regarding OS

Parameter	*P*	HR	95% CI
Age (≥55 vs. <55 y)	<0.001	2.38	1.54–3.68
Sex (male vs. female)	0.16	1.35	0.89–2.06
Karnofsky performance score (<90 vs. ≥90)	0.21	1.72	0.74–4.03
WHO (IV vs. III)	<0.001	2.56	1.61–4.06
MGMT promoter methylation (no vs. yes)	<0.001	2.89	1.83–4.57
Contrast enhancement (yes vs. no)	0.01	2.32	1.23–4.36
Initial treatment (radiotherapy vs. chemotherapy vs. radiochemotherapy)	<0.001	1.87	1.38–2.53
Surgical resection (no vs. yes)	0.90	1.03	0.65–1.63
SUV_{max}/BG	0.27	1.12	0.92–1.35
SUV_{mean}/BG	0.42	1.22	0.76–1.96
BTV	0.11	1.01	1.00–1.02
TTP_{min} (≤12.5 min vs. >12.5 min)	0.001	2.25	1.38–3.67

HR = hazard ratio; CI = confidence interval.
P values were derived from univariate Cox regression for continuous parameters and Log rank test for categoric parameters.

On univariate analysis, WHO III, methylated *MGMT* promoter, young age, absence of contrast enhancement, and chemo- or radiotherapy alone were associated with longer PFS and OS (Table 2). Among the ^{18}F-FET PET parameters, smaller SUV_{max}/BG, smaller BTV, and later TTP_{min} were related to longer PFS. For OS, TTP_{min} correlated significantly with length of survival.

On multivariate analysis, *MGMT* promoter methylation (hazard ratio, 0.51 [95% CI, 0.33–0.81]; $P = 0.003$) and TTP_{min} greater than 12.5 min (hazard ratio, 0.61 [95% CI, 0.38–0.98]; $P = 0.02$) were associated with longer PFS. After stepwise exclusion, the factors younger age, *MGMT* promoter methylation, and TTP_{min} greater than 12.5 min remained favorable predictors for OS, whereas WHO grade, which was intercorrelated with TTP_{min}, was omitted in the last step. In two alternative models with inclusion of either WHO grade or TTP_{min}, both models reached a similar good fit. WHO grade and TTP_{min} were both powerful predictors for OS (hazard ratio for $TTP_{min} \leq 12.5$ vs. > 12.5 min: 2.04 [95% CI, 1.20–3.48], $P = 0.009$; for WHO IV vs. III: 1.73 [95% CI, 1.02–2.93], $P = 0.042$). In the overall group, patients with a TTP_{min} greater than 12.5 min had an OS of 31.8 mo, compared with 15.6 mo for those exhibiting a TTP_{min} of 12.5 min or less ($P = 0.001$; Fig. 2). Detailed results are shown in Table 3.

Patients with a WHO III histology and an early TTP_{min} of 12.5 min or less did not have a significantly different outcome from glioblastoma patients (PFS: 9.3 vs. 10.3 mo, $P = 0.92$; OS: 21.4 vs. 14.2 mo, $P = 0.30$), whereas those with a late TTP_{min} greater than 12.5 min had favorable outcome scores (PFS: 37.4 mo; median OS not reached, Fig. 3). The two WHO III groups exhibiting either early or late TTP_{min} did not differ in sample size, frequency of enhanced tumors on MR imaging, neurosurgical procedure (biopsy vs. surgery), *MGMT* promoter methylation status, applied treatment strategies, or any other PET parameter (SUV_{max}/BG, SUV_{mean}/BG, and BTV). The results were similar in the subgroup of non–contrast-enhancing WHO III gliomas: patients with an early TTP_{min} of 12.5 min or less (10 patients) had an unfavorable outcome compared with those with a late TTP_{min} greater than 12.5 min (9 patients; PFS: 9.8 vs. 37.4 mo, $P < 0.001$; OS: 20.2 mo vs. median not reached, $P < 0.001$).

For the subgroup of WHO IV tumors, increased TTP_{min} was also related to longer survival; however, this finding was less pronounced than in WHO III tumors ($P = 0.08$).

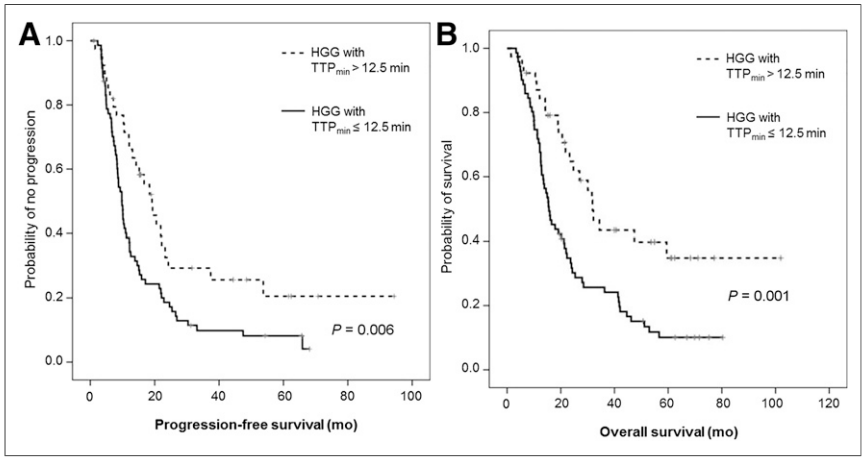


FIGURE 2. Kaplan–Meier estimates for PFS (A) and OS (B) of patients with newly diagnosed astrocytic HGG. Plots show significantly longer PFS and OS for patients with late $TTP_{min} >$ 12.5 min than for patients with short $TTP_{min} \leq 12.5$ min ($P = 0.006$ for PFS and $P = 0.001$ for OS).

DISCUSSION

During the last few years, interest has been increasing in the use of PET with the amino acid analog ^{18}F-FET for glioma imaging, especially dynamic ^{18}F-FET PET. Investigation of individual ^{18}F-FET time–activity curves in the context of tumor grading has been shown to differentiate

Downloaded from jnm.snmjournals.org by on March 14, 2017. For personal use only.

TABLE 3
P Values of Prognostic Factors in Multivariate Analysis Regarding OS

Parameter	*P*	HR	95% CI
Age (≥55 vs. <55 y)	0.015	1.82	1.12–2.94
MGMT promoter methylation (no vs. yes)	<0.001	2.78	1.71–4.50
TTP_{min} (≤12.5 min vs. >12.5 min)	0.009	2.04	1.20–3.48
Age (≥55 vs. <55 y)	0.007	1.95	1.02–3.17
MGMT promoter methylation (no vs. yes)	<0.001	2.73	1.70–4.39
WHO (IV vs. III)	0.042	1.73	1.02–2.93
Age (≥55 vs. <55 y)	0.026	1.73	1.07–2.68
MGMT promoter methylation (no vs. yes)	<0.001	2.62	1.61–4.27
WHO (IV vs. III)	0.150	1.49	0.87–2.56
TTP_{min} (≤12.5 min vs. >12.5 min)	0.023	1.89	1.09–3.22

HR = hazard ratio; CI = confidence interval.
P values were derived from multivariate Cox regression.
The two alternative models, excluding either WHO grade or TTP_{min} as a factor, reached a similar fit. In the model with both factors, TTP_{min} remains significant.

between LGG and HGG (*16–19*). Furthermore, time–activity curves have been helpful for the identification of an oligodendroglial tumor component in low-grade tumors (*25*). Recently, first studies have reported an additional prognostic value for time–activity curves in LGG (*20*) and glioblastomas (*26*). In those studies, the qualitative classification into tumors with increasing versus decreasing time–activity curves revealed an association between uptake kinetics and clinical course, with significantly better outcome for patients with increasing time–activity curves within a single WHO group. To our knowledge, this is the first study investigating the prognostic value of dynamic ^{18}F-FET PET in newly diagnosed, histologically verified HGG, focusing on the quantitative analysis of time–activity curves by evaluating TTP.

Patient survival in the current report was in line with a previously published study (EORTC 26981-22981-NCIC CE3 (*1*)). Our analysis further confirmed well-known prognostic factors such as *MGMT* promoter methylation status, patient age, and the presence of contrast enhancement on the initial MR imaging (*2,27–29*).

Our key finding was that TTP_{min} was the only analyzed ^{18}F-FET PET parameter that had a powerful prognostic impact on PFS and OS after adjustment for the effects of all other variables. Taking into account the intercorrelation seen between WHO grade and TTP_{min}, we tested two alternative prognostic models including either WHO grade or TTP_{min}. We were able to demonstrate that TTP_{min} and WHO grade were similarly good predictors of outcome. To what extent an imbalanced distribution of TTP_{min} values among glioblastoma patients (i.e., a relatively small number of tumors with a long TTP_{min}) might have contributed to the less pronounced impact of TTP_{min}, as compared with WHO III tumors, remains unclear and deserves further evaluation.

Among the WHO III patients, those with an early TTP_{min} of 12.5 min or less had a prognosis not significantly different from that of glioblastoma patients. Outcome for those exhibiting a late TTP_{min} was favorable and remarkably different from that of the poor-prognosis group. Both WHO III glioma subgroups, split by dichotomized TTP_{min}, were homogeneous with regard to all analyzed factors. Moreover, the prognostic impact of TTP_{min} was preserved even for the subgroup of nonenhancing WHO III gliomas only. Apparently, the quantitative analysis of TTP_{min} allows noninvasive identification of patients with WHO III tumors who are at particular risk for early tumor progression and death. This finding can be used in the future for patient stratification and evaluation of risk-adapted treatment strategies for WHO III tumors.

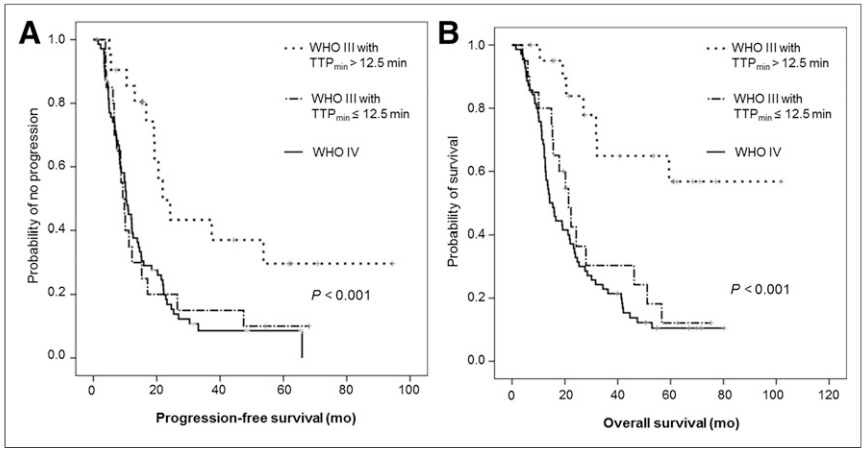


FIGURE 3. Kaplan–Meier estimates for PFS (A) and OS (B) of patients with newly diagnosed astrocytic HGG show significantly increased PFS and OS for WHO III astrocytoma patients with late $TTP_{min} > 12.5$ min ($P < 0.001$ for PFS and OS), whereas those with short $TTP_{min} \leq 12.5$ min had outcome comparable to glioblastoma patients ($P = 0.92$ for PFS and $P = 0.30$ for OS).

The prognostic significance of TTP_{min} agrees with the results of a recently published study in which the shape of time–activity curves (qualitative comparison of increasing time–activity curves, representing

Downloaded from jnm.snmjournals.org by on March 14, 2017. For personal use only.

$TTP_{min} \geq 35$ min, vs. decreasing time–activity curves, characterized by $TTP_{min} < 35$ min) predicted the outcome of patients with newly diagnosed low-grade astrocytoma (*20*). Furthermore, the role of TTP was already described in another study investigating the course of kinetic ^{18}F-FET uptake behavior in LGG, in which a progressively shorter TTP was found during malignant transformation (*21*). Therefore, one might hypothesize that TTP in some way reflects tumor aggressiveness, which, in contrast, cannot be represented by conventional ^{18}F-FET PET parameters such as SUV_{max}/BG and BTV. The pathophysiologic mechanisms being reflected by TTP remain unclear, as the responsible pathway for the different uptake behavior is still not fully clarified. However, as discussed in previous studies (*16,18,25*), one can speculate that two factors play an important role in the uptake dynamics. First, expression of the L-amino acid transporter type 2 promotes bidirectional transport through the cell membrane (*30,31*), hence leading to higher and faster ^{18}F-FET uptake with increasing transporter density. Second, relative cerebral blood flow and tumor perfusion influence tracer delivery (and consequently the amount and speed of tumoral tracer uptake) and subsequent washout after intracellular accumulation of the unbound amino acid analag, which is not incorporated into proteins and may therefore not be trapped intracellularly (*15*). An earlier TTP_{min} may therefore reflect a higher amino acid transporter expression or higher tumor perfusion, which would be in line with the results of other studies reporting that tumor perfusion has prognostic significance (*32–34*). Although a recent study claimed that the descending part of the time–activity curves of ^{18}F-FET uptake does not correlate with perfusion parameters in perfusion-weighted MR imaging, the study found a high correlation with the slope of the increasing part of the time–activity curves (*35*), indicating that tumor perfusion does have an influence to some extent.

The limitations of the study arise from its retrospective design and the differences in treatment management among HGG patients. The latter, however, is due to the lack of a single standardized therapy for newly diagnosed anaplastic astrocytomas. Furthermore, relatively few patients with tumor resection were present in our study, which was based on the management strategy of our neurosurgical center with a highly sophisticated stereotactic biopsy unit. However, because no differences in the neurosurgical procedure (biopsy vs. surgery) or initial treatment were found in the subgroups of WHO III gliomas with early and late TTP_{min}, the comparison of these subgroups seems reliable despite the nonstandardized treatment. Furthermore, population homogeneity regarding the prognostic/predictive factor cytosolic isocitrate dehydrogenase 1/2 mutation was not assessed but would be of great interest in our group of astrocytic HGG patients and should therefore be investigated in future studies. The lack of information concerning 1p/19q status can be considered less relevant, being predominantly associated with oligodendroglial tumors. No central pathology review was performed, but the German Brain Tumor Reference Center in Bonn was consulted for complex cases. Another commonly discussed limiting factor is the histopathologic analysis: most tissue samples were obtained by stereotactic biopsy, which is often considered vulnerable to misdiagnosis (*36*). Because our biopsy planning is PET-based, the probability of missing oligodendroglial tissue with usually high ^{18}F-FET avidity is low, yet although our biopsy planning includes dynamic ^{18}F-FET PET data, which differentiates between low- and high-grade tumor (*19*), a misdiagnosis among HGG cannot be excluded with certainty.

Our study results are promising and need to be confirmed in prospective clinical trials. Because the mechanisms underlying ^{18}F-FET kinetics are not well understood and tumor perfusion might play a role, future studies need to assess the complementary, independent or equivalent information obtained from dynamic ^{18}F-FET PET and perfusion MR imaging data for prognostic evaluation of HGG.

CONCLUSION

Although static ^{18}F-FET PET parameters do not have prognostic significance in patients with newly diagnosed astrocytic HGG, TTP_{min} is an independent prognostic factor with comparable significance to WHO grade: astrocytic HGG with an early TTP_{min} has a significantly worse outcome than astrocytic HGG with later TTP_{min}. The quantitative analysis of TTP_{min} allows noninvasive identification of WHO III glioma patients at particular risk for early tumor progression and death. This finding might be used in the future for patient stratification and individualized risk-adapted treatment strategies for astrocytic WHO III tumors.

DISCLOSURE

The costs of publication of this article were defrayed in part by the payment of page charges. Therefore, and solely to indicate this fact, this article is hereby marked “advertisement” in accordance with 18 USC section 1734. The study was funded in part by the German Glioma Network, supported by German Cancer Aid (Deutsche Krebshilfe 70-3163-Wi 3). No other potential conflict of interest relevant to this article was reported.

REFERENCES

1. Stupp R, Mason WP, van den Bent MJ, et al. Radiotherapy plus concomitant and adjuvant temozolomide for glioblastoma. *N Engl J Med.* 2005;352:987–996.
2. Stupp R, Hegi ME, Mason WP, et al. Effects of radiotherapy with concomitant and adjuvant temozolomide versus radiotherapy alone on survival in glioblastoma in a randomised phase III study: 5-year analysis of the EORTC-NCIC trial. *Lancet Oncol.* 2009;10:459–466.
3. Wick W, Hartmann C, Engel C, et al. NOA-04 randomized phase III trial of sequential radiochemotherapy of anaplastic glioma with procarbazine, lomustine, and vincristine or temozolomide. *J Clin Oncol.* 2009;27:5874–5880.
4. Stupp R, Reni M, Gatta G, Mazza E, Vecht C. Anaplastic astrocytoma in adults. *Crit Rev Oncol Hematol.* 2007;63:72–80.
5. Siker ML, Chakravarti A, Mehta MP. Should concomitant and adjuvant treatment with temozolomide be used as standard therapy in patients with anaplastic glioma? *Crit Rev Oncol Hematol.* 2006;60:99–111.
6. Cairncross G, Wang M, Shaw E, et al. Phase III trial of chemoradiotherapy for anaplastic oligodendroglioma: long-term results of RTOG 9402. *J Clin Oncol.* 2013;31:337–343.
7. Erdem-Eraslan L, Gravendeel LA, de Rooi J, et al. Intrinsic molecular subtypes of glioma are prognostic and predict benefit from adjuvant procarbazine, lomustine, and vincristine chemotherapy in combination with other prognostic factors in anaplastic oligodendroglial brain tumors: a report from EORTC study 26951. *J Clin Oncol.* 2013;31:328–336.
8. Weller M, van den Bent M, Hopkins K, et al. EANO guideline for the diagnosis and treatment of anaplastic gliomas and glioblastoma. *Lancet Oncol.* 2014;15:e395–e403.
9. Hegi ME, Diserens AC, Gorlia T, et al. MGMT gene silencing and benefit from temozolomide in glioblastoma. *N Engl J Med.* 2005;352:997–1003.
10. Hartmann C, Hentschel B, Simon M, et al. Long-term survival in primary glioblastoma with versus without isocitrate dehydrogenase mutations. *Clin Cancer Res.* 2013;19:5146–5157.
11. Ohgaki H, Kleihues P. Genetic profile of astrocytic and oligodendroglial gliomas. *Brain Tumor Pathol.* 2011;28:177–183.
12. Pauleit D, Floeth F, Hamacher K, et al. O-(2-[^{18}F]fluoroethyl)-L-tyrosine PET combined with MRI improves the diagnostic assessment of cerebral gliomas. *Brain.* 2005;128:678–687.
13. la Fougère C, Suchorska B, Bartenstein P, Kreth FW, Tonn JC. Molecular imaging of gliomas with PET: opportunities and limitations. *Neuro-Oncol.* 2011;13:806–819.

Downloaded from jnm.snmjournals.org by on March 14, 2017. For personal use only.

14. Niyazi M, Jansen N, Ganswindt U, et al. Re-irradiation in recurrent malignant glioma: prognostic value of [^{18}F]FET-PET. *J Neurooncol.* 2012;110:389–395.
15. Langen KJ, Hamacher K, Weckesser M, et al. O-(2-[^{18}F]fluoroethyl)-L-tyrosine: uptake mechanisms and clinical applications. *Nucl Med Biol.* 2006;33:287–294.
16. Calcagni ML, Galli G, Giordano A, et al. Dynamic O-(2-[^{18}F]fluoroethyl)-L-tyrosine (F-18 FET) PET for glioma grading: assessment of individual probability of malignancy. *Clin Nucl Med.* 2011;36:841–847.
17. Pöpperl G, Kreth FW, Herms J, et al. Analysis of ^{18}F-FET PET for grading of recurrent gliomas: is evaluation of uptake kinetics superior to standard methods? *J Nucl Med.* 2006;47:393–403.
18. Jansen NL, Graute V, Armbruster L, et al. MRI-suspected low-grade glioma: is there a need to perform dynamic FET PET? *Eur J Nucl Med Mol Imaging.* 2012;39:1021–1029.
19. Kunz M, Thon N, Eigenbrod S, et al. Hot spots in dynamic ^{18}FET-PET delineate malignant tumor parts within suspected WHO grade II gliomas. *Neuro-Oncol.* 2011;13:307–316.
20. Jansen NL, Suchorska B, Wenter V, et al. Dynamic ^{18}F-FET PET in newly diagnosed astrocytic low-grade glioma identifies high-risk patients. *J Nucl Med.* 2014;55:198–203.
21. Galldiks N, Stoffels G, Ruge MI, et al. Role of O-(2-^{18}F-fluoroethyl)-L-tyrosine PET as a diagnostic tool for detection of malignant progression in patients with low-grade glioma. *J Nucl Med.* 2013;54:2046–2054.
22. Eigenbrod S, Trabold R, Brucker D, et al. Molecular stereotactic biopsy technique improves diagnostic accuracy and enables personalized treatment strategies in glioma patients. *Acta Neurochir (Wien).* 2014;156:1427–1440.
23. Louis DN, Ohgaki H, Wiestler OD, et al. The 2007 WHO classification of tumours of the central nervous system. *Acta Neuropathol.* 2007;114:97–109.
24. Grasbon-Frodl EM, Kreth FW, Ruiter M, et al. Intratumoral homogeneity of MGMT promoter hypermethylation as demonstrated in serial stereotactic specimens from anaplastic astrocytomas and glioblastomas. *Int J Cancer.* 2007;121:2458–2464.
25. Jansen NL, Schwartz C, Graute V, et al. Prediction of oligodendroglial histology and LOH 1p/19q using dynamic [^{18}F]FET-PET imaging in intracranial WHO grade II and III gliomas. *Neuro-Oncol.* 2012;14:1473–1480.
26. Tonn JC, Suchorska B, Jansen N, et al. Prognostic value of ^{18}FET positron emission tomography (^{18}FET-PET) for the clinical course in newly diagnosed glioblastoma [abstract]. *J Clin Oncol.* 2013;31(suppl):2045.
27. Habberstad AH, Lind-Landstrom T, Sundstrom S, Torp SH. Primary human glioblastomas: prognostic value of clinical and histopathological parameters. *Clin Neuropathol.* 2012;31:361–368.
28. Weller M, Felsberg J, Hartmann C, et al. Molecular predictors of progression-free and overall survival in patients with newly diagnosed glioblastoma: a prospective translational study of the German Glioma Network. *J Clin Oncol.* 2009;27:5743–5750.
29. Weller M, Stupp R, Hegi ME, et al. Personalized care in neuro-oncology coming of age: why we need MGMT and 1p/19q testing for malignant glioma patients in clinical practice. *Neuro-Oncol.* 2012;14(suppl 4):iv100–iv108.
30. Heiss P, Mayer S, Herz M, Wester HJ, Schwaiger M, Senekowitsch-Schmidtke R. Investigation of transport mechanism and uptake kinetics of O-(2-[^{18}F]fluoroethyl)-L-tyrosine in vitro and in vivo. *J Nucl Med.* 1999;40:1367–1373.
31. Langen KJ, Jarosch M, Muhlensiepen H, et al. Comparison of fluorotyrosines and methionine uptake in F98 rat gliomas. *Nucl Med Biol.* 2003;30:501–508.
32. Bisdas S, Kirkpatrick M, Giglio P, Welsh C, Spampinato MV, Rumboldt Z. Cerebral blood volume measurements by perfusion-weighted MR imaging in gliomas: ready for prime time in predicting short-term outcome and recurrent disease? *Am J Neuroradiol.* 2009;30:681–688.
33. Spampinato MV, Schiarelli C, Cianfoni A, et al. Correlation between cerebral blood volume measurements by perfusion-weighted magnetic resonance imaging and two-year progression-free survival in gliomas. *Neuroradiol J.* 2013;26:385–395.
34. Hirai T, Murakami R, Nakamura H, et al. Prognostic value of perfusion MR imaging of high-grade astrocytomas: long-term follow-up study. *Am J Neuroradiol.* 2008;29:1505–1510.
35. Zhang K, Langen KJ, Neuner I, et al. Relationship of regional cerebral blood flow and kinetic behaviour of O-(2-^{18}F-fluoroethyl)-L-tyrosine uptake in cerebral gliomas. *Nucl Med Commun.* 2014;35:245–251.
36. Glantz MJ, Burger PC, Herndon JE II, et al. Influence of the type of surgery on the histologic diagnosis in patients with anaplastic gliomas. *Neurology.* 1991;41:1741–1744.

Downloaded from jnm.snmjournals.org by on March 14, 2017. For personal use only.

The Journal of NUCLEAR MEDICINE

Prognostic Significance of Dynamic ^{18}F-FET PET in Newly Diagnosed Astrocytic High-Grade Glioma

Nathalie L. Jansen, Bogdana Suchorska, Vera Wenter, Christine Schmid-Tannwald, Andrei Todica, Sabina Eigenbrod, Maximilian Niyazi, Jörg-Christian Tonn, Peter Bartenstein, Friedrich-Wilhelm Kreth and Christian la Fougère

J Nucl Med. 2015;56:9-15.
Published online: December 23, 2014.
Doi: 10.2967/jnumed.114.144675

This article and updated information are available at:
http://jnm.snmjournals.org/content/56/1/9

Information about reproducing figures, tables, or other portions of this article can be found online at:
http://jnm.snmjournals.org/site/misc/permission.xhtml

Information about subscriptions to JNM can be found at:
http://jnm.snmjournals.org/site/subscriptions/online.xhtml

The Journal of Nuclear Medicine is published monthly.
SNMMI | Society of Nuclear Medicine and Molecular Imaging
1850 Samuel Morse Drive, Reston, VA 20190.
(Print ISSN: 0161-5505, Online ISSN: 2159-662X)

© Copyright 2015 SNMMI; all rights reserved.

SNMMI SOCIETY OF NUCLEAR MEDICINE AND MOLECULAR IMAGING